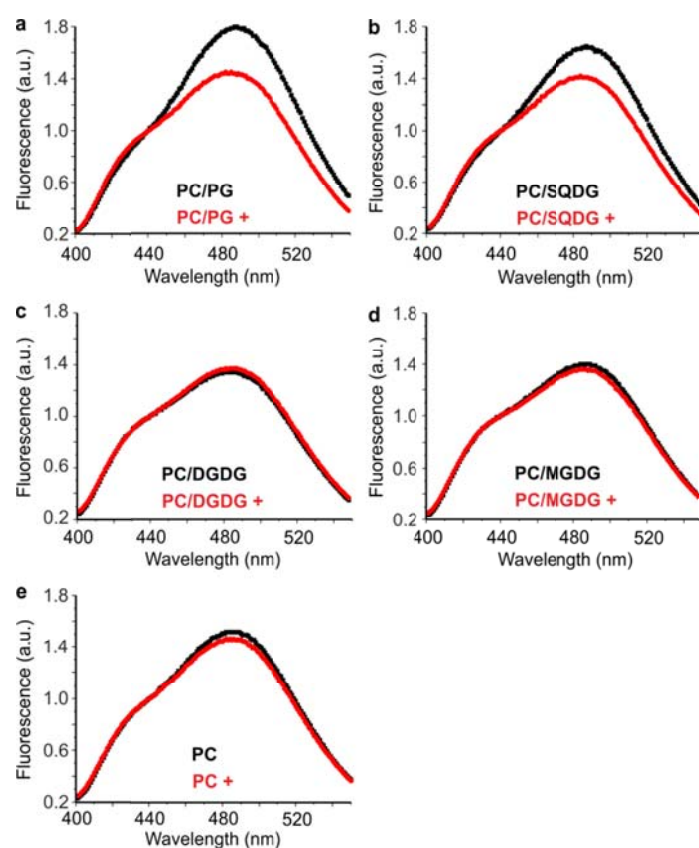


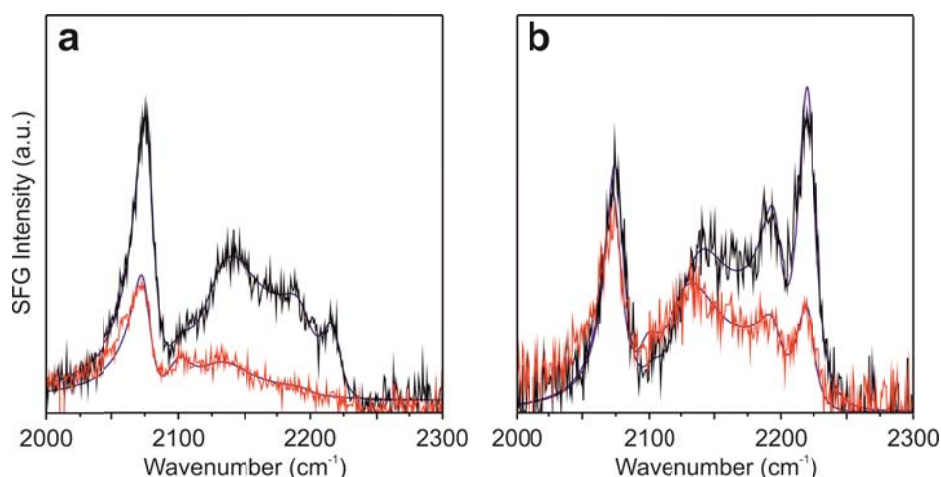
Supplementary Fig. 1: Purification of heterologously expressed IM30.

IM30 was expressed and purified as described in Methods. 2 μg of the isolated protein was analyzed by SDS gel electrophoresis on a 12% SDS polyacrylamide gel. The IM30 sample is inserted between a protein standard, and the molecular masses of the protein standards are indicated on the left. Please note that the IM30 protein frequently runs as a double band on SDS-PAGE gels.



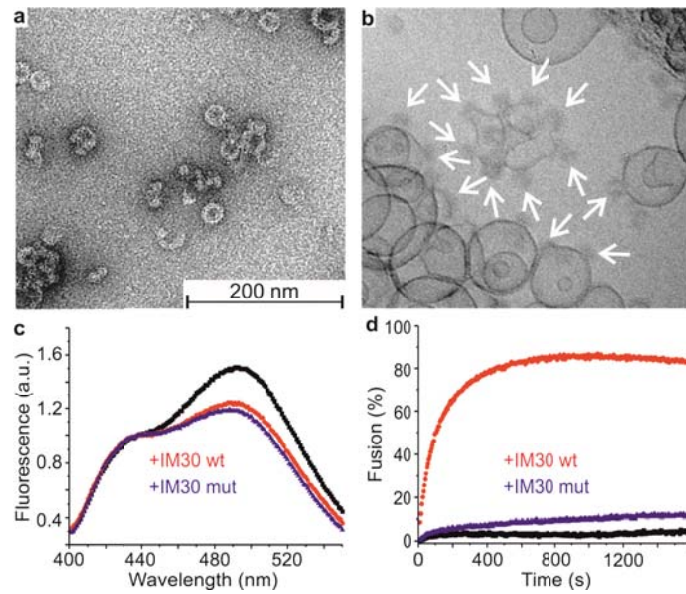
Supplementary Fig. 2: IM30 binds to model membranes in presence of negatively charged TM lipids.

Peripheral binding of IM30 to model membranes was followed by monitoring changes in the Laurdan fluorescence emission after excitation at 350 nm. Fluorescence emission spectra are normalized to the emission at 430 nm and are shown in absence (black) and presence of 2.5 μ M IM30 (red). Decreased fluorescence emission at 490 nm indicates an increased lipid acyl chain order, caused by peripheral binding of IM30. IM30 binding was monitored using PC as a neutral background, to which IM30 does not bind (e), in presence of PG (a), SQDG (b), DGDG (c) or MGDG (d). Only in the case of PG or SQDG-containing membranes, significant changes in Laurdan fluorescence emission were observed. The experiment was performed four times.



Supplementary Fig. 3: IM30 interaction with a lipid monolayer decreases the lipid acyl chain ordering and affects the lipid orientation. The blue lines represent fits of the data.

SFG spectra of deuterated DMPG-D54 (Dimyristoyl-d54-phosphoglycerol) lipid monolayers in presence of 7.5 mM Mg²⁺ were recorded in the C–D stretching range, before (black lines) and after (red lines) addition of IM30. Deuterated lipids were chosen to avoid possible contributions to the signal from IM30. The monolayer was prepared at a pressure of 22 mN/m. IM30 was injected to a total concentration of 5 μM in the sub-phase, after which the system was allowed to equilibrate for 60 minutes. (a) The ssp spectra show a significant reduction of overall signal, which implies the acyl chains are less ordered and aligned after IM30 adsorption. (b) The ppp spectra indicate reorientation of the lipid chains: the ratio of asymmetric methyl stretching modes (near 2220 cm⁻¹) and symmetric methyl modes (near 2070 cm⁻¹) is reduced from 1.3 before to 0.8 after IM30 injection. This indicates a more tilted orientation of the methyl groups in the IM30 covered DMPG-D54 film. Together, ssp and ppp spectra reveal a significant interaction of IM30 with the lipids, causing increased disorder in, and reorientation of the lipid acyl chains.

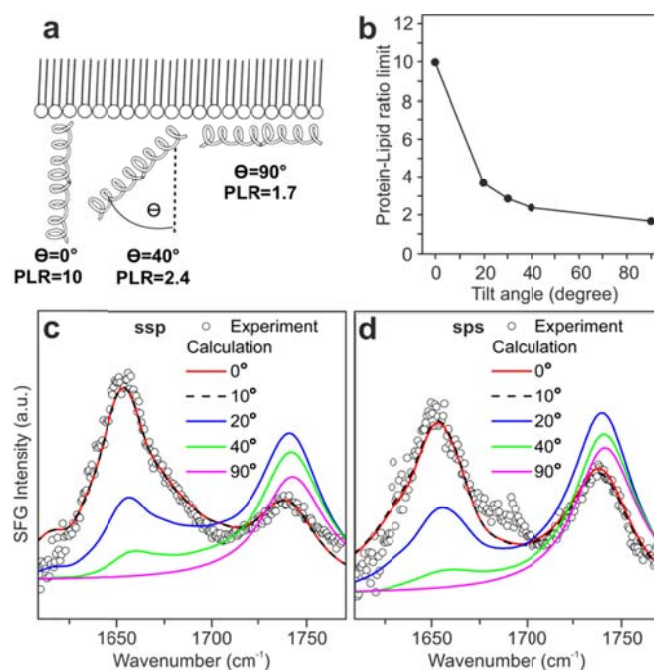


Supplementary Fig. 4: An IM30 mutant that binds to membranes but does not induce membrane fusion.

Three amino acids of the IM30 wild-type sequence have been mutated by site-directed mutagenesis (A76S, A79S, L80A). The mutated protein was expressed and purified as described for the wild-type protein.

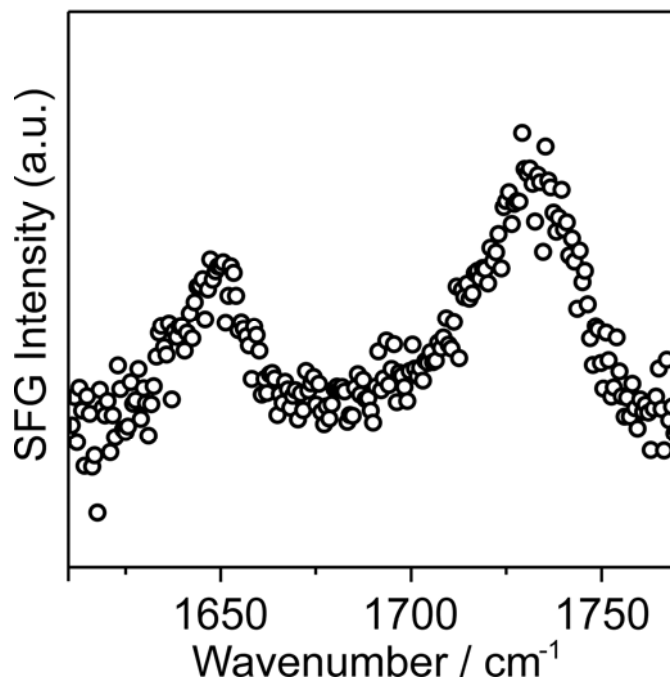
(a) The IM30 mutant forms large oligomeric ring structures as the wild-type protein, as visible in the EM micrographs. (b) Cryo-TEM image of MGDG/PG liposomes in presence of Mg^{2+} and the mutated IM30 taken after 30 minutes of incubation. Arrows indicate extra electron density at the liposome surface, matching in size and shape oligomeric IM30-rings. The magnification was identical in (a) and (b). (c) Peripheral binding of the mutated IM30 (2.5 μ M) to PG-containing MGDG membrane surfaces was followed by monitoring changes in the Laurdan fluorescence emission after addition of IM30 (compare Fig. 1g). Addition of the mutated protein (blue) influenced the fluorescence signal, as observed after addition of the wild-type IM30 protein (red),

suggesting that both IM30-variants have similar membrane binding properties. For comparison, the Laurdan fluorescence signal of membranes in absence of IM30 is shown (black). The experiment was repeated three times. **(d)** MGDG/PG liposomes, containing a donor and an acceptor dye, were mixed with non-labelled liposomes (1:9), and the increase in donor fluorescence emission was monitored over 1600 s after addition of 2.5 μM IM30 in presence of 7.5 mM Mg^{2+} (compare Fig. 3a, b). 0% and 100% fusion rates were determined in control experiments to calculate the fusion efficiency for each sample (see Methods). While the wild-type protein mediated membrane fusion, the mutated IM30 protein was fusion incompetent. The experiment was repeated three times.



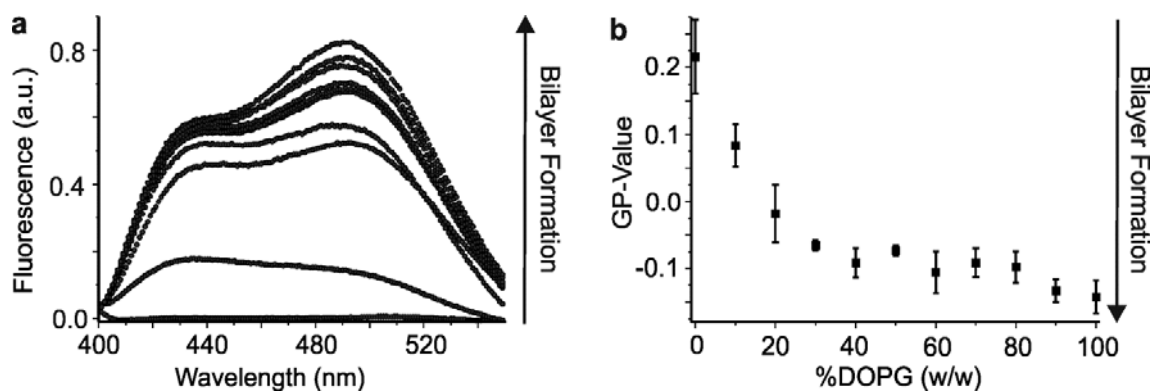
Supplementary Fig. 5: IM30 orientation at lipid monolayer surfaces.

Comparison of experimental and calculated SFG-spectra of IM30 self-assembled onto MGDG/PG (60/40) mixed monolayers for ssp (s polarized SFG, s polarized VIS, p polarized IR) and sps polarization combinations. **(a)** Schematic drawing of the dependency of protein-to-lipid oscillator ratio (PLR) model we used in the calculations. **(b)** PLR upper limits for the tilt angles used in the spectra calculations. **(c)** Comparison of spectra calculated for different orientations of model IM30 units on the monolayers with experimental spectra in ssp-polarization. Calculations, using an average tilt angle of the long helix axis versus the surface normal of 0° - 3° , agree well with the data and are in line with an upright orientation of the IM30 monomers on the membrane surface and a ring-type binding geometry. **(d)** Calculations of SFG-spectra collected with sps-polarization combination. Calculations performed with a tilt angle of 0° - 15° agree well with the data. The experiments were repeated twice.



Supplementary Fig. 6: Less IM30 is bound at the membrane in absence of Mg^{2+} .

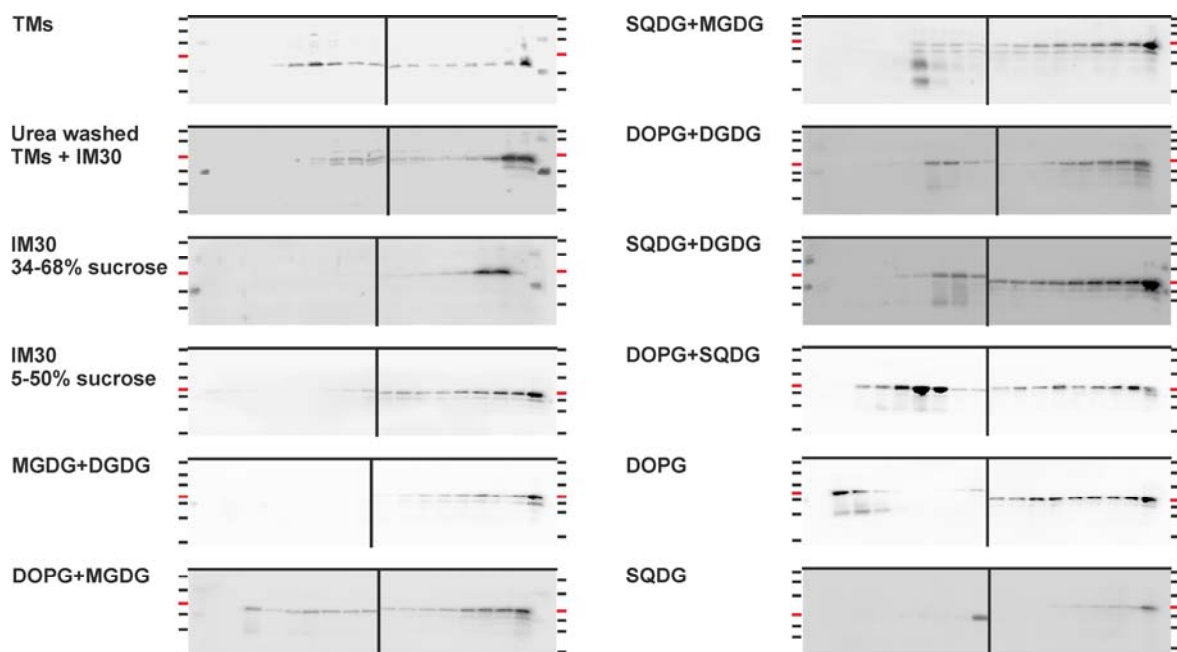
When IM30 is allowed to bind to a lipid monolayer in the absence of Mg^{2+} , a significantly lower IM30 signal is observed in the SFG-spectra (compare Fig. 5c). Thus, Mg^{2+} ions promote the interaction of IM30 with a MGDG/PG monolayer. The experiment was repeated twice.



Supplementary Fig. 7: Formation of stable MGDG-liposomes by addition of DOPG.

The fluorescent probe Laurdan was added to MGDG-lipids, containing increasing DOPG concentrations, to monitor formation of lamellar lipid bilayer structures. (a) The increase in the Laurdan fluorescence emission with increasing DOPG concentrations indicates formation of lipid bilayer structures. In (b), the GP-values are summarized for each % DOPG. Error bars: SD (N=3)

Noteworthy, the DOPG content at which lamellar bilayer structures form (here ~40% DOPG) strongly depends on the buffer conditions, and in the glycerol-containing buffer (SD gradients), lamellar structures formed only at ~50% DOPG.



Supplementary Fig. 8: Uncropped membranes of anti-IM30 immunoblots.

Proteins fractionated by SD gradient centrifugation were separated on 14% SDS-PAGE gels with subsequent immunoblot analysis, using an anti-IM30 antiserum and a peroxidase-coupled anti-rabbit secondary antibody. Due to the high number of samples, the fractions of one SD gradient were loaded on two separated SDS-gels. Equal volumes of the respective fractions were loaded, and after SDS-PAGE, the two corresponding gels were blotted in parallel onto a single membrane for subsequent analysis. Full scans of Western blots are shown. The vertical line marks the boundary of the two individual SDS-gels used for separating the individual fractions of a single SD gradient. The position of the molecular weight markers are indicated on the left or right side of each blot, respectively. The molecular weights of the individual molecular weight marker bands are (from the top): 95, 72, 55, 43 (red), 34, 26 and 17 kDa.